Structural Order in Oxygenated Gallium Nitride Films

N. H. Tran, W. J. Holzschuh, and R. N. Lamb*

Surface Science & Technology, School of Chemical Sciences, University of New South Wales, Sydney 2052, Australia

L. J. Lai and Y. W. Yang

National Synchrotron Radiation Research Center, Hsinchu Science-based Industrial Park, Hsinchu 30077, Taiwan

Received: April 13, 2003; In Final Form: June 23, 2003

Structural order in nanocrystalline, oxygenated GaN thin films (thickness ∼ 500 nm) has been examined. The films were grown using low-pressure chemical vapor deposition of $(CH_3)_2GaN_3$ single source precursor. During deposition, residual oxygen from the vacuum environment was incorporated into the films. Photoemission spectroscopy indicated that oxygen mainly substituted nitrogen during deposition. Long-range X-ray diffraction indicated that the films were oriented along the hexagonal (002) direction when the incorporated concentration of oxygen was lower than 25 atomic % (at. %). Above this, the films were amorphous. The results of angle-dependent near-edge X-ray absorption fine structure facilitated the formation of a short-range structural model, which explained the influences of the oxygen concentration on the long-range order in the films. These studies are useful in understanding the structural evolution in doped-nitride films.

Introduction

The III−V semiconductor GaN exhibits a large direct band gap of 3.4 eV and can be used as light emitting in the visible−UV regions. A common problem in producing single crystalline (i.e., epitaxial) GaN films concerns the selection of substrate materials with comparable lattice constants and crystal symmetry.[1] Polycrystalline films have, however, been grown on a variety of substrates using methods such as molecular beam epitaxy and chemical vapor deposition. During growth, residual oxygen is a common impurity that alters the electrical properties of the films. The incorporation of oxygen can facilitate the formation of free electron concentration within GaN crystallites, which leads to formation of *n*-type semiconducting films.[2−4] Theoretical studies of the oxygen incorporation into GaN and other nitrided films have been reported.[5]

In this paper, we examine the structural order in the nanocrystalline GaN films with the presence of various oxygen impurity concentrations. The films were grown by single source chemical vapor deposition of the organo-metallic $(CH_3)_2GaN_3$ precursor.[6] We employed X-ray diffraction to examine the long-range order within the films while the complementary short-range order was analyzed using near-edge X-ray absorption fine structure (NEXAFS).

Experimental Section

The deposition of GaN films on Si(100) substrates was carried out in a high vacuum chamber with a background pressure of $\sim 4 \times 10^{-7}$ Torr. The partial pressure of $(CH_3)_2GaN_3$ precursor was $\sim 5 \times 10^{-5}$ Torr during growth. The substrate temperatures ranged from 400 to 600 °C, resulting in oxygen concentrations within films decreasing from ∼50 to 10 at. %. Deposition for 3 h resulted in a film thickness of ∼500 nm.

The chemical composition of the films was determined using a Kratos XSAM800 X-ray photoemission spectrometer (XPS) with an unmonochromated Mg Kα source. X-ray diffraction was performed using a PW 3040/60 X′Pert Pro Diffractometer with an unmonochromated Cu Kα source. Near-edge X-ray absorption fine structure was carried out at beamline 24A, Synchrotron Radiation Research Centre, Hsinchu, Taiwan.[7] The total electron yield absorption spectra were measured at normal and grazing incident conditions with the angle of incident X-ray and sample surface normal at 0° and 70°, respectively. Prior to the measurements, samples were heated in the ultrahigh vacuum analysis chamber at ∼200 °C for 5 min in order to minimize the adventitious surface contaminants.

Results and Discussion

Figure 1 shows the XPS survey scan of a GaN film from the chemical vapor deposition of $(CH_3)_2GaN_3$ single source. In particular, the binding energy of Ga $2p_{3/2}$ and N 1s photoelectrons were assigned at $E_b \sim 1117.1$ eV and 396.9 eV, respectively. The O 1s photoelectrons were assigned at binding energy of $E_b \sim 531.1$ eV. The chemical composition as a function of substrate temperatures is shown in Figure 2. The atomic concentration of gallium remained virtually unchanged at ∼47 at. % within the temperature range of 400−600 °C. At 400 °C, the atomic concentration of oxygen was detected at ∼50 at. %. The oxygen atomic concentration decreased sharply at 450 °C as the concentration of nitrogen increased.

Figure 3 shows the XPS region scan of Ga $2p_{3/2}$ photoelectrons of the GaN standard reference and the films with variation of oxygen concentration. The binding energy of Ga $2p_{3/2}$ photoelectrons in the films with oxygen lower than 25 at. %

* Corresponding author. Fax: 612 9662 1697. E-mail: r.lamb@unsw.edu.au.

10.1021/jp034990x CCC: $25.00
Published on Web 07/31/2003

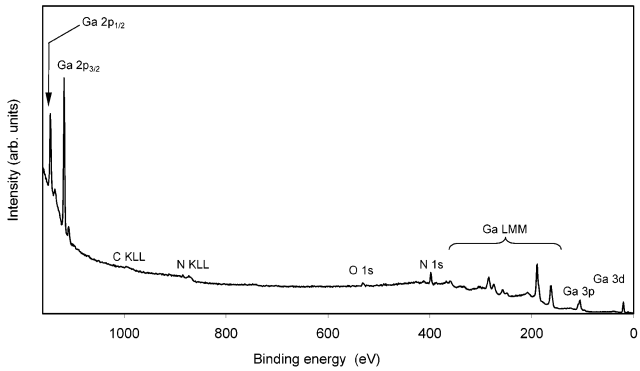

Figure 1. XPS survey scan of an oxygenated GaN film grown using chemical vapor deposition of $(CH_3)GaN_3$ single source precursor.

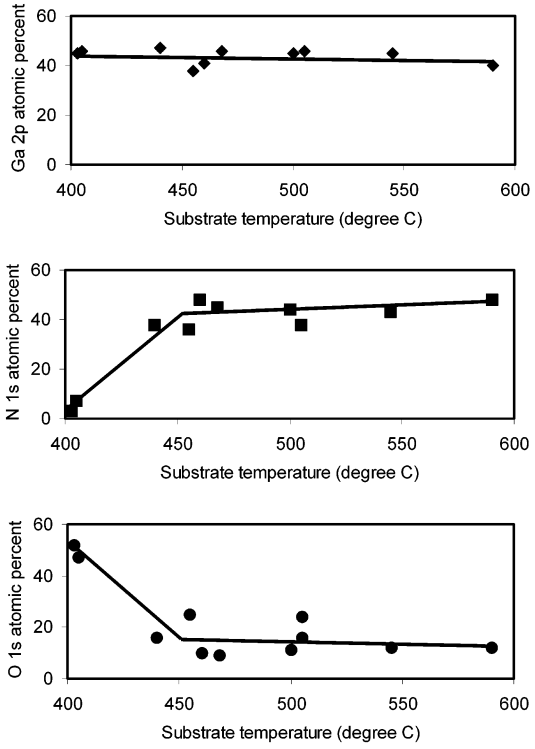

Figure 2. Atomic concentration of Ga $2p_{3/2}$, N 1s and O 1s photoelectrons in SS CVD GaN thin films as a function of substrate temperature.

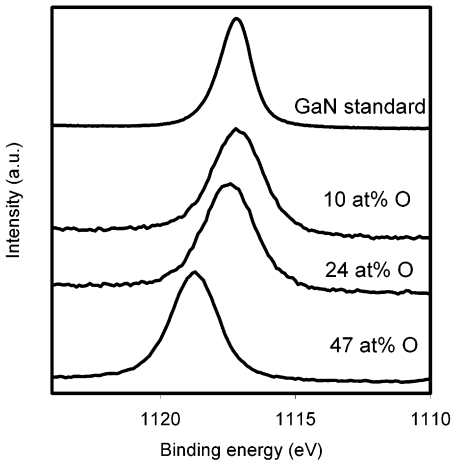

Figure 3. XPS region scan of Ga $2p_{3/2}$ photoelectrons of GaN reference standard and thin films with different oxygen concentration.

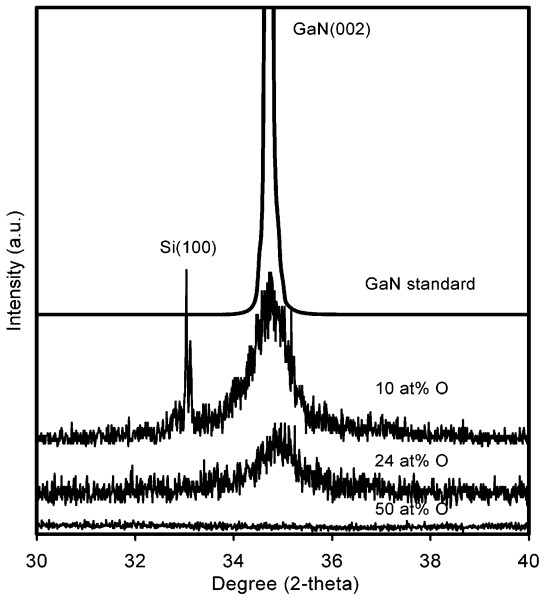

Figure 4. XRD of GaN reference standard and thin films with varying oxygen concentration. In the XRD of the film with ~10 at. % oxygen, the doublet at 2θ ~33° was attributed to the underlying Si(100) substrate, and its intensity was dependent on the alignment of Si in the diffractometer.

was similar to that of the reference. For the film with ~50 at. % oxygen, the Ga $2p_{3/2}$ binding energy was measured at 1118.7 eV. This is 1.6 eV higher than for the film with 10 at. % oxygen, and results from the higher electronegativity of the oxygen increasing the ionic character of the gallium bonds and consequently leading to an increase in the 2p binding energies.[8]

The XPS results indicated that oxygen predominantly substituted nitrogen, resulting in more thermodynamically stable Ga−O species (the enthalpy of formation, $\Delta_f H$, of Ga−N and Ga−O bonds is −110 kj/mol-Ga and −545 kj/mol-Ga, respectively).[9] Formation of Ga−O was favored during deposition at relatively low temperatures in these experiments (i.e., lower than 600 °C). Temperatures lower than 750 °C facilitated the formation of poorly desorbed gallium atoms, which were more mobile and easily trapped the residual oxygen from gas phase.[10−12]

Additional evidence of the formation of Ga−O bonds is obtained via the optical properties of the films. These films appear to be transparent as they show the color bands consistent with the interference effect. The UV−visible reflectance spectra of the films with oxygen content lower than 25 at. % showed a sharp cutoff in transparency at ~348 nm that corresponds to a direct band gap of $E_g \sim 3.55$ eV. This is slightly higher than that of bulk GaN ($E_g \sim 3.40$ eV) and in agreement with the photoluminescence (PL) results of the polycrystalline GaN films ($E_g \sim 3.50$ eV) prepared by the thermal reaction of ammonia with Ga_2O_3 layer.[13] Also the band gap of Ga_2O_3 is ~4.7 eV.[14] The relatively high band gap in our UV measurements is attributed to the Ga−O bonds in the films that therefore become slightly more insulating compared to bulk GaN.

The oxygen substitution significantly influenced the crystallographic properties of the films, as shown in Figure 4. The XRD patterns of the films with oxygen lower than 25 at. % were similar to that of the reference. However, these films resulted in a broad, low signal-to-noise ratio peak with relative intensity being much lower compared to the reference. The detection of the single peak at $2\theta = 34.8°$ indicated that the films were crystalline and oriented preferentially along the hexagonal (002) direction. The average crystallite sizes in these films estimated from the fwhm values of the XRD peaks were

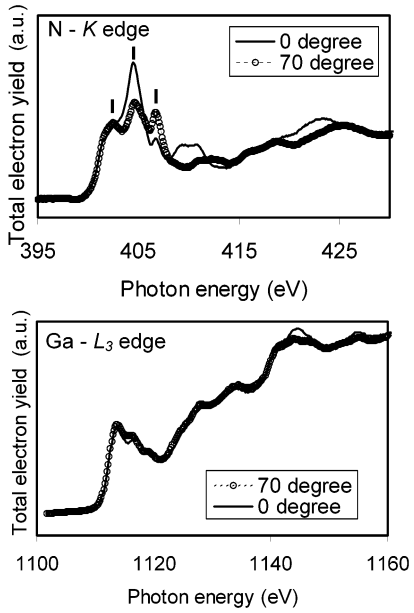

Figure 5. N *K*-edge and Ga L_3-edge NEXAFS of GaN reference standard at grazing and incident conditions.

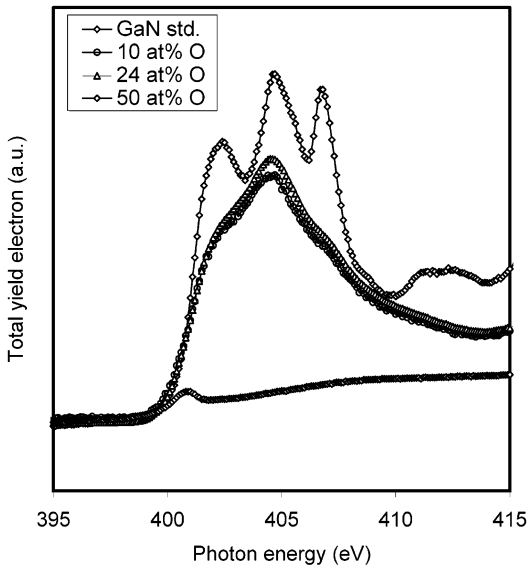

Figure 6. N *K*-edge grazing incident NEXAFS for GaN standard and thin films with varying oxygen concentration.

varied between 15 and 25 nm. In addition, the film with oxygen at ~50 at. % was amorphous.

XRD provided information concerning the structural order within the films with oxygen lower than 25 at. %. However, the films with oxygen of ~50 at. % were beyond the limitation of the XRD measurements. To understand the structural information within these films, the complementary technique of NEXAFS was used to investigate the films. Figure 5 shows the N *K*-edge and Ga L_3-edge NEXFAS spectra of the reference at the normal and grazing conditions. The N 1s absorption edge was recorded at 402.7 eV.[15−20] The significance of the angular dependency concerned the intensity enhancement of the peaks at 404.8 and 406.8 eV, as the measurements were carried out at normal and grazing incidence, respectively. The peak intensity at 402.7 eV was also slightly enhanced at grazing incidence. According to the dipole selection rule (i.e., an electron transition requires a change in angular momentum quantum number of $\Delta l = \pm 1$),[21] the N 1s electrons will be promoted to the nearest empty *p* states, similar to that observed for O 1s electrons from various transition metal oxides.[22] Since information concerning the orbitals perpendicular to the film surface will be maximized at grazing incident geometry, we interpreted the peaks at 404.8 and 406.8 eV as being related to the transitions between 1s and $2p_{x,y}$ orbitals and between 1s and $2p_z$ orbitals, respectively.[15−20]

The molecular structure of hexagonal GaN consisted of slightly distorted GaN_4 tetrahedra with three Ga−N bonds involving the hybridized $2p_{x,y}$ orbitals (in-plane bonds), and a slightly longer bond involving the hybridized $2p_z$ orbitals (out-of-plane bond), parallel to the hexagonal (002) direction. The observed angular dependency during N *K*-edge measurements confirmed the above long-range XRD results with the GaN reference being oriented preferentially along the hexagonal (002) direction. In addition, the relative intensity of the peak at 404.8 eV directly monitored the concentration of the in-plane bonds, while the intensity of the 406.8 eV peak monitored the out-of-plane bonds.[15−20] In contrast, the Ga L_3-edge transitions were virtually independent of the incident angles, as the spectra mainly concerned the electronic transitions to the unoccupied *s* valence states.[18,20]

Figure 6 shows the N *K*-edge grazing incident NEXAFS normalized spectra of the oxygenated GaN films and the reference standard. For the crystalline films with oxygen lower than 25 at. %, the absorption edge and the in-plane components were recorded at 402.7 and 404.8 eV, respectively, similar to that of the standard. The intensity of the peak attributed to the out-of-plane components was decreased dramatically relative to that of the reference and was not well resolved. In particular, their spectra show the presence of a broad shoulder at the energy range between 405 and 410 eV. These results indicated that oxygen preferentially substituted the out-of-plane components of GaN_4 tetrahedra. Such substitution is energetically favored as the (002) plane has the lowest surface free energy, similar to that of the hexagonal zinc oxide.[23] For the amorphous film with oxygen concentration ~50 at. %, the absorption edge was shifted to lower energy of 401.1 eV, while the out-of-plane and in-plane peaks were not well defined. This indicated that the corresponding out-of-plane and in-plane components of GaN_4 tetrahedra were substituted by oxygen.

The interaction of oxygen was previously interpreted via a kinetic process, in which oxygen acted as a shallow donor that facilitated the formation of mobile gallium serving as a deep acceptor (V_{Ga}).[2,5,12] These donor−acceptor interactions were energetically favored and led to formation of the defect complexes ($V_{Ga} - O_N$) segregating at the dislocation sites or the grain boundaries of GaN crystallites (O_N represented the nitrogen-substituting oxygen). The above NEXAFS results give rises to a local structural model in which the oxygen substitution allows gallium to retain its tetrahedral structure (Figure 7). For this, tetrahedron is the low energy form of Ga−O bonds in gallium oxide,[24] and there is only a slight difference between the atomic distance of Ga−O (1.82 Å) and Ga−N (1.94 Å).[25] During film growth with oxygen concentration lower than 25 at. %, the competing interactions of nitrogen and oxygen with the dangling bonds parallel to the (002) axis led to formation of the out-of-plane components consisting of a mixture of Ga−O and Ga−N bonds. This led to formation of a number of distorted GaN_3O tetrahedra within the GaN network. It is expected that the formation of GaN_3O reduced the concentration of the out-of-plane Ga−N bonds but did not influence greatly the bulk structure. Together with the remaining GaN_4 tetrahedra, they allowed the formation of oxygenated GaN films with well-defined hexagonal structure (Figure 4).

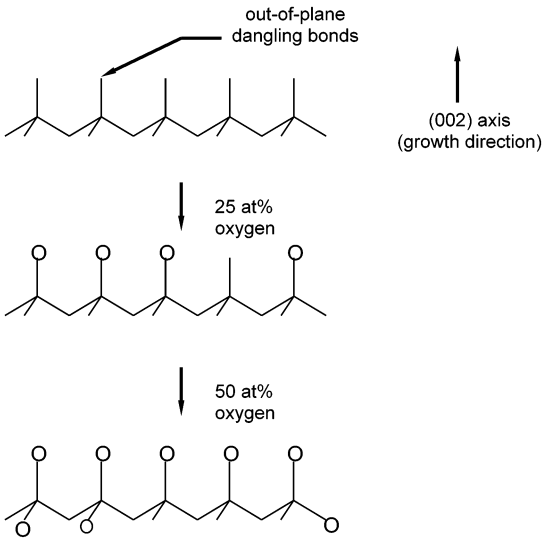

Figure 7. Simple cluster model consisting of five tetrahedral units with Ga being the core atoms. For the oxygen concentration lower than 25 at. %, a maximum number of four oxygen atoms could substitute nitrogen atoms, preferentially at the out-of-plane positions. For the oxygen concentration lower than 50 at. %, a maximum number of eight oxygen atoms could substitute at both the out-of-plane and in-plane positions.

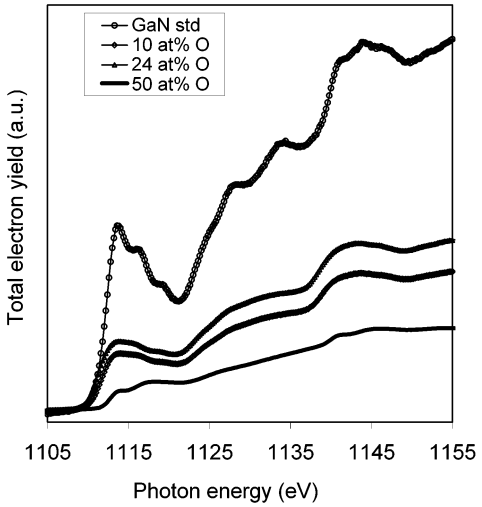

Figure 8. Ga L_3-edge grazing incident NEXAFS of GaN standard and thin films with varying oxygen concentration.

The Ga L_3-edge measurements also support the idea that, despite oxygen substitution in the lattice, gallium remained tetrahedrally bonded as shown in Figure 8. The spectra of the films with oxygen concentration lower than 25 at. % were similar to that of the reference, with the absorption edge at ~1114 eV. For this, the Ga *K*-edge results of gallium oxide indicated that the absorption edge was recorded at ~10.375 and 10.379 keV for the tetrahedral and octahedral environments, respectively.[24] The increase in energy absorption was attributed to the larger electronegativity of the octahedral gallium.

During film growth with oxygen concentration higher than 25 at. %, the oxygen substitution at both out-of-plane and in-plane positions led to formation of GaN_3O and also GaN_2O_2 species as a highly distorted tetrahedra (Figure 7). For the film with oxygen concentration of ~50 at. %, ideally all GaN_4 tetrahedra were partly substituted. This gave rise to a large residual stress which was released by formation of the amorphous films. Formation of highly distorted gallium tetrahedra was supported through the Ga L_3-edge measurement for the film with oxygen ~50 at. % (Figure 8). The energy shift of the absorption edge was similar to the tetrahedral reference and only its relative intensity was slightly changed.

Summary

During chemical vapor deposition of GaN, the competing interactions of residual oxygen in the vacuum chamber and nitrogen in the precursor with gallium lead to formation of mixed Ga−O and Ga−N bonds. The incorporation of residual oxygen with concentration lower than 25 at. % resulted in formation of the crystalline, hexagonal (002) films with the average crystallite sizes between 15 and 25 nm. The films with oxygen concentration of ~50 at. % were amorphous. During film growth, oxygen preferentially substituted the bonds parallel to the (002) direction. The results facilitated the formation of a local structural model, which explained the influences of the oxygen concentration on the long-range order in the films. These studies are useful in understanding the dependency of oxygen and other dopants on the local structures of nitrided films.

Acknowledgment. This work was performed at the Australian National Beamline Facility with support from the Australian Synchrotron Research Program. The authors thank L. Fan and A. Buckley for supporting data acquisition.

References and Notes

(1) Rigby, P. *Nature* **1997**, *388* (6637), 29−30 (and references therein).

(2) Wetzel, C.; Suski, T.; Ager, J. W., III; Weber, E. R.; Haller, E. E.; Fischer, S.; Meyer, B. K.; Molnar, R. J.; Perlin, P. *Phys. Rev. Lett.* **1997**, *78* (20), 3923−3926.

(3) Oila, J.; Ranki, V.; Kivioja, J.; Saarinen, K.; Hautojärvi, P.; Likonen, J.; Baranowski, J. M.; Pakula, K.; Suski, T.; Leszczynski, M.; Grzegory, I. *Phys. Rev. B* **2001**, *63* (045205), 1−8.

(4) Toth, M.; Fleischer, K.; Phillips, M. R. *Phys. Rev. B* **1999**, *59* (3), 1575−1578.

(5) Mattila, T.; Nieminen, R. M. *Phys. Rev. B* **1996**, *54* (23), 16676−16682.

(6) Atwood, D. A.; Jones, R. A.; Cowley A. H.; Atwood, J. L.; Bott, S. G. *J. Organomet. Chem.* **1990**, *394*, C6−C8. Lakhotia, V.; Neumayer, D. A.; Cowley, A. H.; Jones, R. A.; Ekerdt, J. G. *Chem. Mater.* **1995,** *7*, 546−552.

(7) Lai, L. J.; Tseng, P. C.; Yang, Y. W.; Chung, S. C.; Song, Y. F.; Cheng, N. F.; Chen, C. C.; Chen, C. T.; Tsang, K. L. *Nucl. Instrum. Methods Phys. Res. A* **2001**, 467−468, 586−588.

(8) Wolter, S. D.; Luther, B. D.; Waltemyer, D. L.; Önneby, C.; Mohney, S. E.; Molnar, R. J. *Appl. Phys. Lett.* **1997**, *70* (16), 2156−2158.

(9) Lide, D. R. *CRC Handbook of Chemistry and Physics*, 83rd ed.; CRC Press: Boca Raton, FL, 2002.

(10) Guha, S.; Bojaczuk, N. A.; Kisker, D. W. *Appl. Phys. Lett.* **1996**, *69*, 2879−2881.

(11) Evans, K. R.; Lei, T.; Jones, C. R. *Solid State Electron.* **1997**, *41*, 339.

(12) Elsner, J.; Jones, R.; Heggie, M. I.; Stich, P. K.; Haugk, M.; Frauenheim, T.; Oberg, S.; Briddon, P. R. *Phys. Rev. B* **1998**, *58*, 12571−12574.

(13) Yang, Y. G.; Ma, H. L.; Xue, C. S.; Hao, X. T.; Zhuang, H. Z.; Ma, J. *Physica B* **2003**, *325*, 230−234.

(14) Nakano, Y.; Kachi, T.; Jimbo, T. *Appl. Phys. Lett.* **2003**, *82* (15), 2443−2445.

(15) Katsini, M.; Paloura, E. C.; Moustakas, T. D. *Appl. Phys. Lett.* **1996**, *69* (27), 4206−4208.

(16) Katsikini, M.; Paloura, E. C.; Antonopoulos, J.; Bressler, P.; Moustakas, T. D. *J. Cryst. Growth* **2001**, *230*, 405−409.

(17) Lawniczak-Jablonska, K.; Iwanowski, R. J.; Demchenko, I. N.; Boettcher, T.; Einfeldt, S.; Hommel, D.; Cortes, R.; Perera, R. C. C. *J. Alloys Compd.* **2001**, *328*, 77−83.

(18) Chiou, J. W.; Mookerjee, S.; Rao, K. V. R.; Jan, J. C.; Tsai, H. M.; Asokan, K.; Pong, W. F.; Chien, F. Z. *Appl. Phys. Lett.* **2002**, *81* (18), 3389−3391.

(19) Lübbe, M.; Bressler, P. R.; Braun, W.; Kampen, T. U.; Zahn, D. R. T. *J. Appl. Phys.* **1999**, *86* (1), 209−213.

(20) Lawniczak-Jablonska, K.; Suski, T.; Gorczyca, I.; Chritensen, N. E.; Attenkofer, K. E.; Perera, R. C. C.; Gullikson, E. M.; Underwood, J. H.; Ederer, D. L.; Weber, Z. L. *Phys. Rev. B* **2000**, *61* (24), 16623−16632.

(21) Bianconi, A.; Marcelli, A. In *Synchrotron Radiat. Res., Adv. Surf. Interface Sci.* **1992**, *1*, 63, and references therein.

(22) Chen, J. G. *Surf. Sci. Rep.* **1997**, *30*, 1−152.

(23) Tran, N. H.; Hartmann, A.; Lamb, R. N. *J. Phys. Chem. B* **1999**, *103* (21), 4264−4268 (and references therein).

(24) Nishi, K.; Shimizu, K.; Takamatsu, M.; Yoshida, H.; Satmusa, A.; Tanaka, T.; Yoshida, S.; Hattori, T. *J. Phys. Chem. B* **1998**, *102*, 10190−10195.

(25) Downs, A. J. *Chemistry of Aluminium, Gallium, Indium and Thallium*, 1st ed.; Blackie Academic & Professional: Glasgow, 1993. Nakamura, S.; Fasol, G. *The Blue Laser Diode*; Springer-Verlag: Berlin, 1997.